(Preprint) AAS 23-230

MULTI-BODY PRESCRIBED SPACECRAFT DYNAMICS SUBJECT TO ACTUATOR INPUTS

Leah Kiner[*], Cody Allard[†] and Hanspeter Schaub[‡]

The kinematics of spacecraft components undergoing prescribed motion is of interest when considering articulated solar panels or actuated motion platforms. However, simulating a component's trajectory given a general combination of actuator inputs presents challenges when the relationship between actuator and component states is not directly known. This paper introduces a method of formulating the rotational kinematics of a two-axis gimbal actuated sequentially by two stepper motors. Given a series of step commands, the motor and gimbal state history are analytically determined using a provided motor-to-gimbal angle lookup table. The formulation is implemented and validated in a gimbal thruster pointing scenario.

INTRODUCTION

Early in the mission development phase, the complex dynamical behavior of candidate spacecraft designs must be modeled to assess their ability to meet mission science and maneuverability requirements. For example, consider a spacecraft with articulated solar panels,[1] or an electric thruster mounted on a motion platform to change the body-relative thrust vector.[2] Here, three-dimensional solid models are traditionally used to both realize and analyze complex spacecraft components in these first stages of development processes. These solid models store fundamental kinematic information describing how rigid spacecraft components can move with respect to a specified spacecraft base of reference given a series of actuator inputs. The predominant challenge in utilizing these solid models lies in the uniqueness of each solid model. Number of actuators, number of component degrees of freedom, and geometric constraints between actuators and the actuated component are all challenges inherent in developing general methods to construct an actuated spacecraft component's trajectory.

The dynamics of such rigid spacecraft components whose motion is restricted to follow particular trajectories in three-dimensional space are referred to as being *prescribed*, and hence these objects are said to undergo *prescribed motion*. NASA's Cassini spacecraft seen in Fig. (1) consisted of several prescribed components including an articulated main engine, a one degree of freedom (DOF) probe relay antenna, and a high-precision two DOF scan platform.[3] The Space Station Remote Manipulator System (SSRMS) a.k.a. the "Canadarm" consists of eight links and seven active joints

[*]Graduate Research Assistant, Ann and H.J. Smead Department of Aerospace Engineering Sciences, University of Colorado Boulder, Colorado Center For Astrodynamics Research, Boulder, CO, 80303 USA. leah.kiner@colorado.edu

[†]Guidance, Navigation and Control Engineer, Laboratory for Atmospheric and Space Physics, University of Colorado Boulder, Boulder, CO, 80303 USA

[‡]Professor and Department Chair, Schaden Leadership Chair, Ann and H.J. Smead Department of Aerospace Engineering Sciences, University of Colorado, Boulder, 431 UCB, Colorado Center for Astrodynamics Research, Boulder, CO, 80309. AAS Fellow, AIAA Fellow.

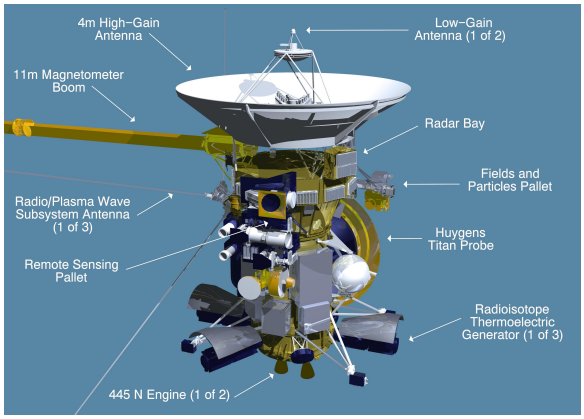

Figure 1. Cassini spacecraft.*

whose motion can be commanded either through pre-programmed trajectories or individually using prescribed angles.[3,4] Other common examples of prescribed spacecraft components include stepper motors, actuated platforms, gimballed thrusters, and servo-ed sensors. Moreover, the dynamics of such prescribed bodies are assumed to be one-way coupled with the other rigid spacecraft components, meaning their motion impacts the dynamics of the spacecraft system, but not vice versa; as precise servo sub-systems are used to achieve the spacecraft body-relative positioning. The validity of this assumption has to be analyzed based on the bandwidth and performance of the servo controller.

One common approach of dealing with the dynamics of traditional actuated bodies such as reaction control thrusters, reaction wheels, or magnetic actuators is to simply neglect the actuator dynamics altogether if the response is assumed to be fast enough.[5] However, for high-precision attitude control problems where actuator dynamics significantly impact the spacecraft dynamics or controller performance, this assumption is not sufficient. Accordingly, Kristiansen and Hagen developed both a first and second order generalized MIMO linear model and incorporated mechanical time delays into the actuator dynamics.[5] Similarly, other existing work seeks to analyze the robust stabilization of nonlinear systems subject to unmodeled actuator and sensor dynamics.[6–8] However, because this work focuses on actuated bodies undergoing prescribed motion, the dynamics of these bodies are assumed to be obtainable over the entire spectrum of actuation inputs, hence removing the need to analyze uncertainty in the actuator dynamics.

For robotic manipulators consisting of chains of translational and rotational joints connected by rigid links, one common approach for deriving the kinematic relationship between joints is forward kinematics, where four Denavit and Hartenberg parameters (D-H parameters)[9] are required to derive a compact and generalized transformation between robotic joints.[10,11] However, for more complex spacecraft components whose geometry is not a simple collection of joints and links, a method of deriving the kinematic relationship between actuation inputs and resulting three-dimensional motion is more complicated to resolve.

In practice, actuator manufacturers usually provide lookup tables that relate motor inputs to actuator outputs. These tables are specific to the type of actuator and may not contain the full kinematic state information of the actuated body. Some lookup tables may only provide scalar angular infor-

*https://solarsystem.nasa.gov/resources/12943/diagram-of-the-cassini-spacecraft/

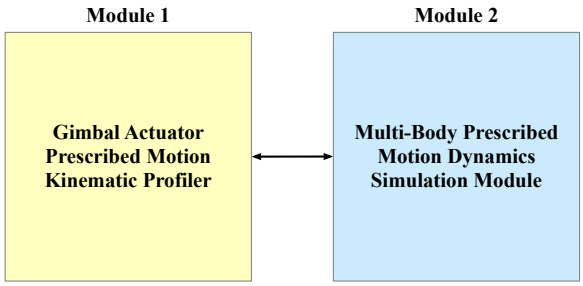

Figure 2. Modules required for gimbal thruster pointing scenario simulation.

mation where the mapping from actuator inputs to the actuated body's kinematic states is unclear. Oftentimes interpolation must be used between data points given in such a lookup table to construct the actuator's kinematic states. Lookup tables may also not provide any state rate information, requiring further approximations to be made to construct the actuator kinematics. To this end, several challenges are presented when determining the full translational, rotational, and attitude kinematic states of complex spacecraft components from three-dimensional solid models.

This paper expands upon prior work in multibody prescribed motion dynamics where the dynamics of a rigid spacecraft hub with a connected secondary rigid body undergoing prescribed motion were derived and validated using the Basilisk[†] open-source astrodynamics simulation software package.[12,13] A general two-axis gimbal actuated sequentially by two stepper motors is considered in this paper. The actuator is mounted to a fixed location on the rigid spacecraft hub, meaning its translational, rotational, and attitude states are all described relative to a single base frame. Further, the translational states of the actuator are considered fixed. As a result, only the rotational states of the actuator must be determined to simulate its prescribed motion.

The sequence of modules required to simulate the prescribed gimbal motion in a spacecraft dynamics scenario is outlined in Fig. (2). The solution methodology presented in this work focuses on development of Module 1, which solves for the gimbal's prescribed kinematic rotational states given a series of motor step count commands. Module 2 takes the gimbal's prescribed states as inputs and simulates a spacecraft dynamics scenario where the gimbal actuator is connected to a rigid spacecraft hub. Module 2 was implemented in Basilisk and its development was described in previous work.[12] The approach taken in this work to develop Module 1 utilizes a motor-to-gimbal angle lookup table provided by a two-axis gimbal manufacturer. Linear interpolation is used between discreet data points given in the lookup table to solve for the gimbal attitude for any combination of motor states. The developed formulation is validated in a gimbal thruster pointing scenario. If desired, the resulting kinematic states of the actuator can be given as inputs to Module 2, where the effect of the thruster pointing on the overall spacecraft motion can be simulated and analyzed.

PROBLEM STATEMENT

Spacecraft Model

This work considers a spacecraft consisting of a rigid central hub and an appended kinematically prescribed actuator body. The spacecraft geometry of interest is illustrated in Fig. (3). The required coordinate frames for the system dynamics derivation are as follows. The inertial reference frame

[†]`https://hanspeterschaub.info/basilisk`

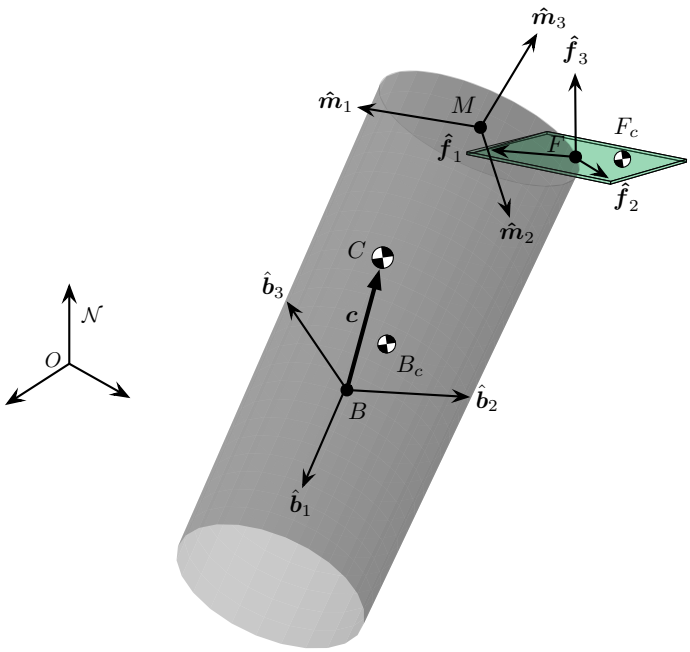

Figure 3. Spacecraft geometry, variables, and coordinate frames used for this derivation.

is indicated by $\mathcal{N} : \{N, \hat{\boldsymbol{n}}_1, \hat{\boldsymbol{n}}_2, \hat{\boldsymbol{n}}_3\}$. The spacecraft body frame $\mathcal{B} : \{B, \hat{\boldsymbol{b}}_1, \hat{\boldsymbol{b}}_2, \hat{\boldsymbol{b}}_3\}$ describes the motion of the rigid hub. The origin of this frame is located at a hub-fixed point B. The hub-fixed point B_c is the hub center of mass location. The body frame of the actuator $\mathcal{F} : \{F, \hat{\boldsymbol{f}}_1, \hat{\boldsymbol{f}}_2, \hat{\boldsymbol{f}}_3\}$ describes the motion of the prescribed body attached to the spacecraft hub through a mount interface. The origin of the actuator body frame is located at the point F that is actuator-fixed. The point F_c is the center of mass of the actuator. The mount frame $\mathcal{M} : \{M, \hat{\boldsymbol{m}}_1, \hat{\boldsymbol{m}}_2, \hat{\boldsymbol{m}}_3\}$ is fixed with respect to the spacecraft hub and is introduced as a matter of kinematic convenience.

The actuator prescribed motion is defined relative to the body-fixed mount frame to simplify the associated kinematic description. Point M indicates the origin of the mount frame. The spacecraft center of mass C relative to point B is indicated by $\boldsymbol{c}$. Note that points B, B_c, C, M, F and F_c need not be necessarily coincident.

It is assumed that the translational and rotational states of the actuator with respect to the spacecraft hub are known and prescribable. These prescribed states of interest are provided in Table (1), along with the other body-fixed parameters for this problem set up. The prescribed parameter $'$ notation indicates a time derivative taken in the actuator frame $\mathcal{F}$. Because the two bodies considered are rigid bodies, the center of mass location of each body with respect to the origin of their respective body frames are known. Moreover, the position and attitude of the mount frame relative to the hub frame are known because the mount frame is specified as fixed to the hub. The angular velocity of the mount frame with respect to the hub frame $\boldsymbol{\omega}_{\mathcal{M}/\mathcal{B}}$ is zero for all time.

Actuator Model

The actuator considered in this work is a two-axis gimbal, meaning two successive angles are used to describe the attitude of the gimbal relative to the mount frame. These angles are referred to as "tip" and "tilt" angles in this work. A general two-axis actuator applicable to this work is shown in

Table 1. Prescribed states of interest.

Body-Fixed Parameters	Prescribed Parameters
$\mathbf{r}_{B_c/B}$	$\mathbf{r}_{F/M}$
$\mathbf{r}_{F_c/F}$	$\mathbf{r}'_{F/M}$
$\mathbf{r}_{M/B}$	$\mathbf{r}''_{F/M}$
$\boldsymbol{\sigma}_{\mathcal{M}/\mathcal{B}}$	$\boldsymbol{\sigma}_{\mathcal{F}/\mathcal{M}}$
	$\boldsymbol{\omega}_{\mathcal{F}/\mathcal{M}}$
	$\boldsymbol{\omega}'_{\mathcal{F}/\mathcal{M}}$

Figure 4. Two-axis actuated platform.

Fig. (4). The gimbal attitude is controlled by two actuated stepper motors. Both motors rotate with step angle $\Delta\theta$, requiring each motor to take $N_s = \frac{360^\circ}{\Delta\theta}$ steps per revolution. As a result, there are N_s^2 possible combinations of motor positions for a general two-motor system with no constraints. Manufacturers of gimbal actuators commonly provide a lookup table containing combinations of stepper motor angles and the corresponding gimbal tip and tilt angles. The notations used in this work for the stepper motor and gimbal angles are given in Table (2).

Depending on the actuator constraints, the stepper motors could be commanded to move simultaneously, individually, or a combination of both cases. This work assumes each motor is actuated independently to achieve the desired gimbal attitude pointing. This assumption is necessary for straightforward interpolation of the given lookup table data when the motor step size is not identical to the lookup table step size. The inputs to the stepper motors are two step commands, identifying the number of steps each motor must take to complete the desired attitude maneuver. For each motor step, the gimbal correspondingly moves through a sequential tip and tilt motion. The rotation axes for the tip and tilt motion are typically specific and dependent on the type of gimbal actuator chosen.

Motor Input to Gimbal Platform Kinematic States Methodology

Recall that Fig. (2) outlines the two fundamental modules required to simulate the gimbal actuator's prescribed motion and incorporate its dynamics into a full spacecraft gimbal thruster pointing scenario. The focus of this work is the development of Module 1, which solves for the gimbal's

Table 2. Stepper motor and gimbal angle notation.

Motor 1 Angle	θ_1
Motor 2 Angle	θ_2
Gimbal Tip Angle	ψ
Gimbal Tilt Angle	ϕ

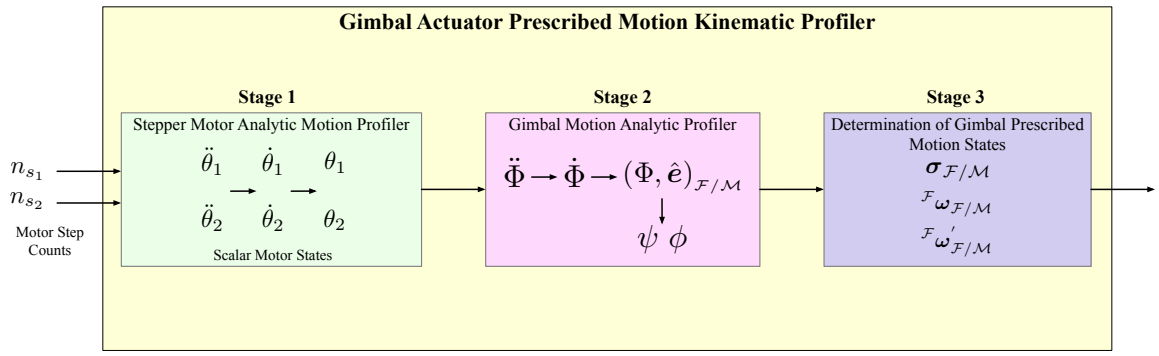

Figure 5. Solution methodology diagram.

prescribed kinematic rotational states given a series of motor step count commands. The process used to develop the gimbal kinematic profiler is separated into three stages seen in Fig. (5). Stage 1 receives the motor step counts and analytically determines the stepper motors' scalar rotational states. A bang-bang acceleration profile applying the maximum allowable motor acceleration is used to construct the motor state history for each step. Next, Stage 2 analytically profiles the gimbal's motion using a motor-to-gimbal angle lookup table. Spherical linear interpolation is used between discreet angles if the motor angle step size is not equal to the table-provided step size. The initial and final gimbal attitude for each motor step is determined and expressed using Principal Rotation Parameters (PRPs), where a second bang-bang acceleration profile is used to drive the gimbal through the required relative PRP angle during a fixed motor step time Δt. Stage 2 also determines the gimbal tip and tilt angle history for the motor step. The output of Stage 2 is a time history of the gimbal's PRPs, the PRP angle rate, and acceleration. Finally, Stage 3 formulates the gimbal's prescribed motion rotational states specified in Table (1). The following section discusses in detail the formulation of each stage of Module 1.

GIMBAL ACTUATOR PRESCRIBED MOTION KINEMATICS

Stage 1: Stepper Motor Analytic Motion Profiler

The first stage required to prescribe the gimbal's kinematic motion seen in Fig. (5) is to construct the stepper motors' rotational motion profiles given two step count command inputs. Given the initial motor angles, initial gimbal angles, and the gimbal reference angles, a step count command for each motor is determined that will drive the gimbal to the specified reference attitude. For gimbal tip and tilt reference angles ψ_{ref} and ϕ_{ref}, the corresponding motor reference angles θ_{ref_1} and θ_{ref_2}

are found using the provided lookup table. The next section discusses how to interpolate between angles if the desired angles are not directly available in the lookup table. The required motor step counts are:

$$n_{s_1} = \frac{\theta_{\text{ref}_1} - \theta_{0_1}}{\Delta\theta} \qquad n_{s_2} = \frac{\theta_{\text{ref}_2} - \theta_{0_2}}{\Delta\theta} \tag{1}$$

Note that the stepper motors are actuated independently in this work to drive the gimbal to the desired final attitude. If motor 1 is chosen to actuate first it will complete n_{s_1} steps before motor 2 begins to actuate and take n_{s_2} steps.

For a single motor step, the required angular rotation is achieved using a bang-bang acceleration profile. Given the motor's maximum angular acceleration magnitude $\ddot{\theta}_{\text{max}}$, this value is applied positively for the first half of the step and negatively for the second half of the step. During the acceleration phase, the motor angle rate increases linearly, reaching a maximum value halfway through the step. During the deceleration phase, the motor angle rate decreases linearly and returns to zero. The resulting angular profile is parabolic. The trajectory is concave-up for first half of the step and concave-down for the second half.

Clearly, the stepper motor states can be determined entirely analytically. First, the time required to take one motor step $\Delta\theta$ is determined:

$$\Delta t = 2\sqrt{\frac{\Delta\theta}{\ddot{\theta}_{\text{max}}}} = t_f - t_0 \tag{2}$$

The switch time t_s indicates when the acceleration is alternated:

$$t_s = t_0 + \frac{\Delta t}{2} \tag{3}$$

The equations used to obtain the motor states for the first half of the step are:

$$\ddot{\theta}(t) = \ddot{\theta}_{\text{max}} \tag{4a}$$

$$\dot{\theta}(t) = \ddot{\theta}_{\text{max}}(t - t_0) \tag{4b}$$

$$\theta(t) = \frac{\Delta\theta}{2}\frac{(t - t_0)^2}{(t_s - t_0)^2} + \theta_0 \tag{4c}$$

During the deceleration phase, the motor equations are:

$$\ddot{\theta}(t) = -\ddot{\theta}_{\text{max}} \tag{5a}$$

$$\dot{\theta}(t) = \ddot{\theta}_{\text{max}}(t - t_f) \tag{5b}$$

$$\theta(t) = -\frac{\Delta\theta}{2}\frac{(t_s - t_f)^2}{(t - t_f)^2} + \theta_{\text{ref}} \tag{5c}$$

Equations (4)-(5) are the complete analytic expressions describing the motor states for an individual motor step; therefore, development of stage 1 is complete. Note that for each successive motor step, the parameters t_0, t_s, and t_f must be updated to reflect the advancement of time. Accordingly, the above equations can be used given any number of motor step counts to drive the gimbal to the reference attitude.

Stage 2: Gimbal Motion Analytic Profiler

The second phase to prescribe the motion of the gimbal actuator seen in Fig. (5) is to profile the gimbal's trajectory for any number of motor step counts. The profiled gimbal motion should be generalized so that it can be applied to any combination of motor steps. Given the scalar motor state history from Stage 1, Stage 2 produces a gimbal trajectory using Principal Rotation attitude Parameters (PRPs). PRPs are closely related to the Principal Rotation Vector (PRV) attitude vector $\boldsymbol{\gamma}$:[14]

$$\boldsymbol{\gamma} = \Phi \hat{\boldsymbol{e}} \tag{6}$$

The PRPs $(\Phi, \hat{\boldsymbol{e}})$ represent the angle and rotation axis components of the PRV; where the attitude of one frame relative to another is described by a rotation about a principal axis $\hat{\boldsymbol{e}}$ by a principal angle Φ.[14] In addition to obtaining the gimbal's attitude history, this stage also determines the gimbal angles ψ, ϕ, the scalar principal rotation angle rate $\dot{\Phi}$, and acceleration $\ddot{\Phi}$. The PRP information is output to Stage 4 and used to determine the prescribed motion states of the gimbal seen in Table (1). The development of this stage is broken up into 3 steps outlined in the following section.

The first step to profile the gimbal's motion is to determine the initial and final gimbal PRPs for each motor step. Because the motor state history was analytically determined in Stage 1, the initial and final motor angles can be used to determine the initial and final PRPs:

$$(\theta_1, \theta_2)_0 \rightarrow (\Phi, \hat{\boldsymbol{e}})_0 \qquad\qquad (\theta_1, \theta_2)_f \rightarrow (\Phi, \hat{\boldsymbol{e}})_f \tag{7}$$

The mapping above is often not directly known; however it is common for gimbal actuator manufacturers to provide a lookup table from motor angles to gimbal tip and tilt angles:

$$\theta_1, \theta_2 \rightarrow \psi, \phi \tag{8}$$

The motor angles are discretized by a constant step size $\delta\theta$. If either the initial or final set of motor angles coincides with a row in the lookup table, the provided gimbal tip and tilt angles can be immediately converted to PRPs. A straightforward method treats the gimbal angles as Euler Angles. The Euler Angles represent a sequential two-axis rotation from the mount frame reference to the gimbal frame. These Euler angles can then be transformed to a direction cosine matrix (DCM), followed by a transformation to PRPs.

The Euler angle sequence for a two-axis rotation is denoted $(i\text{-}j) = (\psi, \phi)$, indicating that the gimbal first performs a tip rotation about the $\mathcal{M}$ frame axis i ($\hat{\boldsymbol{m}}_i$) by ψ degrees, followed by a tilt rotation about the intermediate/gimbal $\mathcal{F}$ frame axis j ($\hat{\boldsymbol{f}}_j$) by ϕ degrees. The Euler angle sequence is mapped to the corresponding rotation matrix using the following expression:

$$(i\text{-}j) = (\psi, \phi) = [C_j(\phi)][C_i(\psi)] = [\mathcal{FM}] \tag{9}$$

where $[C_i(\psi)]$ and $[C_j(\phi)]$ are single-axis DCMs corresponding to the tip and tilt rotations, respectively. For example, a $(1\text{-}2) = (\psi, \phi)$ sequential rotation is expressed as:

$$[C_2(\phi)][C_1(\psi)] = \begin{bmatrix} \cos\phi & 0 & -\sin\phi \\ 0 & 1 & 0 \\ \sin\phi & 0 & \cos\phi \end{bmatrix} \begin{bmatrix} 1 & 0 & 0 \\ 0 & \cos\psi & \sin\psi \\ 0 & -\sin\psi & \cos\psi \end{bmatrix} \tag{10}$$

$$[\mathcal{FM}] = \begin{bmatrix} \cos\phi & \sin\phi\sin\psi & -\sin\phi\cos\psi \\ 0 & \cos\psi & \sin\psi \\ \sin\phi & -\cos\phi\sin\psi & \cos\phi\cos\psi \end{bmatrix} \tag{11}$$

Table 3. Provided lookup table for motor to gimbal angles.

Motor 1 Angle	Motor 2 Angle	Gimbal Tip Angle	Gimbal Tilt Angle
$\theta_{i-1,1}$	$\theta_{i-1,2}$	ψ_{i-1}	ϕ_{i-1}
$\theta_{i,1}$	$\theta_{i,2}$	ψ_i	ϕ_i
θ_1	θ_2	ψ	ϕ
$\theta_{i+1,1}$	$\theta_{i+1,2}$	ψ_{i+1}	ϕ_{i+1}

The obtained DCM can be transformed to a PRV using the transformation:[14]

$$[\tilde{\gamma}] = -\ln([\mathcal{FM}]) = \sum_{n=1}^{\infty} \frac{(-1)^{n+1}}{n} (I_{3\times 3} - [\mathcal{FM}])^n \tag{12}$$

Note Eq. (12) is singular for $\Phi = \pm\pi$. The tilde matrix operator $[\tilde{\boldsymbol{v}}]$ denotes:

$$[\tilde{\boldsymbol{v}}] = \begin{bmatrix} 0 & -v_3 & v_2 \\ v_3 & 0 & -v_1 \\ -v_2 & v_1 & v_0 \end{bmatrix} \tag{13}$$

The principal rotation axis and angle information can extracted from the found PRV:

$$\Phi = |\boldsymbol{\gamma}| \tag{14a}$$

$$\hat{\boldsymbol{e}} = \frac{\boldsymbol{\gamma}}{\Phi} \tag{14b}$$

However, it is likely the case that the true motor step angle $\Delta\theta$ is several orders of magnitude smaller than the provided lookup table motor step size ($\delta\theta \gg \Delta\theta$). Table (3) illustrates a section of a typical lookup table provided by a gimbal manufacturer. The row containing red parameters indicates a scenario where certain motor angles are not incorporated into the lookup table data. In this case, interpolation is required to obtain an estimate of the gimbal PRPs. Assuming that each motor individually actuates enables linear interpolation to be used when the motor angles do not match a row in the provided lookup table. When interpolation is required, the two neighboring rows bounding the current motor angles must be selected and transformed to PRPs.

The PRPs associated with the smaller and larger angles of the actuated motor are denoted $(\Phi_1, \hat{\boldsymbol{e}}_1)$ and $(\Phi_2, \hat{\boldsymbol{e}}_2)$, respectively. The desired interpolated gimbal PRPs are denoted $(\Phi, \hat{\boldsymbol{e}})_{\text{ref}}$. To most simply interpolate, a relative principal rotation axis and angle is determined so only the principal angle must be interpolated. To determine the relative PRPs, the bounding PRPs must be subtracted:

$$(\Phi, \hat{\boldsymbol{e}})_{\text{rel}} = (\Phi_2, \hat{\boldsymbol{e}}_2) - (\Phi_1, \hat{\boldsymbol{e}}_1) \tag{15}$$

where[14]

$$\Phi_{\text{rel}} = 2\cos^{-1}\left(\cos\frac{\Phi_2}{2}\cos\frac{\Phi_1}{2} + \sin\frac{\Phi_2}{2}\sin\frac{\Phi_1}{2}\right)\hat{\boldsymbol{e}}_2 \cdot \hat{\boldsymbol{e}}_1 \tag{16a}$$

$$\hat{\boldsymbol{e}}_{\text{rel}} = \frac{\cos\frac{\Phi_1}{2}\sin\frac{\Phi_2}{2}\hat{\boldsymbol{e}}_2 - \cos\frac{\Phi_2}{2}\sin\frac{\Phi_1}{2}\hat{\boldsymbol{e}}_1 + \sin\frac{\Phi_2}{2}\sin\frac{\Phi_1}{2}\hat{\boldsymbol{e}}_2 \times \hat{\boldsymbol{e}}_1}{\sin\frac{\Phi}{2}} \tag{16b}$$

Using the actuated motor angles and the relative principal rotation angle, the relative interpolated angle Φ_{int} is found between zero and Φ_{rel}:

$$\Phi_{\text{int}} = \frac{\Phi_{\text{rel}}(\theta_j - \theta_{i,j})}{\theta_{i+1,j} - \theta_{i,j}} \tag{17}$$

where $j = 1$ when motor 1 is actuated and $j = 2$ when motor 2 is actuated. The relative interpolated PRPs are therefore obtained as $(\Phi_{\text{int}}, \hat{\boldsymbol{e}}_{\text{rel}})$. It should be noted that these PRPs represent a *relative* gimbal attitude, meaning they must be added to the lower PRPs $(\Phi_1, \hat{\boldsymbol{e}}_1)$ found in the lookup table to obtain the correct interpolated gimbal PRPs:

$$(\Phi, \hat{\boldsymbol{e}})_{\text{ref}} = (\Phi_{\text{int}}, \hat{\boldsymbol{e}}_{\text{rel}}) + (\Phi_1, \hat{\boldsymbol{e}}_1) \tag{18}$$

where[14]

$$\Phi_{\text{ref}} = 2\cos^{-1}\left(\cos\frac{\Phi_1}{2}\cos\frac{\Phi_{\text{int}}}{2} - \sin\frac{\Phi_1}{2}\sin\frac{\Phi_{\text{int}}}{2}\right)\hat{\boldsymbol{e}}_1 \cdot \hat{\boldsymbol{e}}_{\text{int}} \tag{19a}$$

$$\hat{\boldsymbol{e}}_{\text{ref}} = \frac{\cos\frac{\Phi_{\text{int}}}{2}\sin\frac{\Phi_1}{2}\hat{\boldsymbol{e}}_1 + \cos\frac{\Phi_1}{2}\sin\frac{\Phi_{\text{int}}}{2}\hat{\boldsymbol{e}}_{\text{int}} + \sin\frac{\Phi_1}{2}\sin\frac{\Phi_{\text{int}}}{2}\hat{\boldsymbol{e}}_1 \times \hat{\boldsymbol{e}}_{\text{int}}}{\sin\frac{\Phi}{2}} \tag{19b}$$

At this step in the formulation of Stage 2, both initial and final gimbal PRPs $(\Phi, \hat{\boldsymbol{e}})_0$ and $(\Phi, \hat{\boldsymbol{e}})_f$ are known. The next step Stage 2 involves profiling the gimbal trajectory between the initial and final PRPs for a single motor step. A bang-bang acceleration profile similar to the one developed in Stage 1 to define the stepper motor motion is used to drive the gimbal from its initial attitude to the final attitude. Because the motor step time Δt is fixed, the gimbal is required to move through the angle Φ_{ref} in time Δt. The acceleration required for the gimbal to complete the maneuver in the correct time is:

$$\alpha = \frac{4\Phi_{\text{ref}}}{\Delta t^2} \tag{20}$$

The equations used to obtain the gimbal principal rotation angle, angle rate, and acceleration for the first half of the motor step are:

$$\ddot{\Phi}(t) = \alpha \tag{21a}$$

$$\dot{\Phi}(t) = \alpha(t - t_0) \tag{21b}$$

$$\Phi(t) = \frac{\Phi_{\text{ref}}}{2}\frac{(t - t_0)^2}{(t_s - t_0)^2} \tag{21c}$$

During the deceleration phase, the equations are:

$$\ddot{\Phi}(t) = -\alpha \tag{22a}$$

$$\dot{\Phi}(t) = \alpha(t - t_f) \tag{22b}$$

$$\Phi(t) = -\frac{\Phi_{\text{ref}}}{2}\frac{(t_s - t_f)^2}{(t - t_f)^2} + \Phi_{\text{ref}} \tag{22c}$$

The profiled gimbal PRP attitude is denoted $(\Phi, \hat{\boldsymbol{e}})_{\mathcal{F}/\mathcal{M}}$ where $\hat{\boldsymbol{e}} = \hat{\boldsymbol{e}}_{\text{ref}}$. The second step in Stage 2 completes the formulation of the gimbal PRPs, principal angle rates, and accelerations for a single motor step. Equations (21) and (22) are expressed generally so that the gimbal trajectory can be constructed for any number of motor steps. Recall that the parameters t_0, t_s, and t_f must be updated to reflect the advancement of time for each successive motor step.

The final step to complete development of Stage 2 involves determining the gimbal tip and tilt angle trajectories for a single motor step. Although the tip and and tilt angles are not required in Stage 3 to determine the gimbal's prescribed motion states, it is useful to use these angles to visualize the gimbal trajectory in two-dimensional space. For gimbal actuators that have limited ranges of motion, checking the tip and tilt angles is useful to ensure the gimbal is functioning within its proper range of motion.

Using the gimbal's PRP attitude trajectory, the DCM corresponding to each PRP set can be determined:[14]

$$[\mathcal{FM}] = e^{-\Phi[\tilde{\boldsymbol{e}}]} = [I_{3\times 3}]\cos\Phi - \sin\Phi[\tilde{\boldsymbol{e}}] + (1-\cos\Phi)\hat{\boldsymbol{e}}\hat{\boldsymbol{e}}^T \tag{23}$$

Treating the gimbal tip and tilt angles as Euler angles once again enables application of inverse trigonometric functions to elements of the determined DCM to obtain the tip and tilt angles. For example, assuming a (1-2) = (ψ, ϕ) rotation yields the DCM result seen in Eq. (9). The gimbal angles are simply:

$$\psi = \tan^{-1}\left(\frac{[\mathcal{FM}]_{23}}{[\mathcal{FM}]_{21}}\right) \qquad \phi = \tan^{-1}\left(\frac{[\mathcal{FM}]_{31}}{[\mathcal{FM}]_{11}}\right) \tag{24}$$

Equations (21 - 24) complete the development of Stage 2. The gimbal PRP attitude trajectory, principal angle rates, and accelerations are next given as inputs to Stage 3 to determine the gimbal's prescribed motion states.

Stage 3: Determination of Gimbal Prescribed Motion States

The third stage required to obtain a full kinematic profile for a prescribed gimbal actuator is to transform the gimbal's profiled attitude trajectory, principal angle rates and accelerations to the prescribed states outlined in Table (1). Recall that the translational parameters are assumed to be zero and unaffected by the stepper motor motion for this actuator model.

First, the gimbal's attitude relative to the mount frame is determined in terms of Modified Rodrigues parameters (MRPs). Formulated through a stereographic projection of the four-dimensional quaternion set onto a three-dimensional hyperplane, this attitude set is chosen because it is a minimal coordinate set with no constraints in $\mathbb{R}^3$ space.[14] Other popular choices of attitude parameters include Euler parameters (quaternions), direction cosine matrices (DCM) or Euler angles. The MRP describing the gimbal attitude relative to the mount frame reference is denoted $\boldsymbol{\sigma}_{\mathcal{F}/\mathcal{M}}$.

The time history of PRPs developed in Stage 2 are directly mapped to MRP space using the following transformation:

$$\boldsymbol{\sigma}_{\mathcal{F}/\mathcal{M}} = \begin{pmatrix}\sigma_1\\ \sigma_2\\ \sigma_3\end{pmatrix} = \tan\left(\frac{\Phi}{4}\right)\hat{\boldsymbol{e}} \tag{25}$$

Next, the gimbal angular velocity and angular acceleration relative to the mount frame can be obtained using the known principal rotation axes and the principal angle rates and accelerations. Note that the notation used for a body frame time derivative of a vector $\boldsymbol{v}$ is denoted $\boldsymbol{v}^{'}$; therefore, $\boldsymbol{\omega}^{'}_{\mathcal{F}/\mathcal{M}}$ designates the $\mathcal{F}$-frame time derivative of $\boldsymbol{\omega}_{\mathcal{F}/\mathcal{M}}$.

$$^{\mathcal{F}}\boldsymbol{\omega}_{\mathcal{F}/\mathcal{M}} = \dot{\Phi}\hat{\boldsymbol{e}} \tag{26a}$$

$$^{\mathcal{F}}\boldsymbol{\omega}^{'}_{\mathcal{F}/\mathcal{M}} = \ddot{\Phi}\hat{\boldsymbol{e}} \tag{26b}$$

Equations (25-26) are the expressions required to fully prescribe the gimbal's kinematic motion and integrate the gimbal states into a spacecraft simulation software simulation.

SPACECRAFT SYSTEM PRESCRIBED MOTION DYNAMICS

The second module seen in Fig. (2) is required to simulate the prescribed gimbal motion in a spacecraft dynamics scenario. The translational and rotational equations of motion for the spacecraft system with a general prescribed body attached to the spacecraft hub illustrated in Fig. (3) are derived in previous work[12] and are implemented in Module 2. The results are presented in Eqs. (27) and (28) below.

$$m_{\text{sc}}\ddot{\boldsymbol{r}}_{B/N} + m_{\text{sc}}[\dot{\tilde{\boldsymbol{\omega}}}_{\mathcal{B}/\mathcal{N}}]\boldsymbol{c} = \sum \boldsymbol{F}_{\text{ext}} - m_{\text{P}}\boldsymbol{r}^{''}_{F_c/B} - 2m_{\text{sc}}[\tilde{\boldsymbol{\omega}}_{\mathcal{B}/\mathcal{N}}]\boldsymbol{c}^{'} - m_{\text{sc}}[\tilde{\boldsymbol{\omega}}_{\mathcal{B}/\mathcal{N}}]^2\boldsymbol{c} \tag{27}$$

$$\begin{aligned} m_{\text{sc}}[\tilde{\boldsymbol{c}}]\ddot{\boldsymbol{r}}_{B/N} + [I_{\text{sc},B}]\dot{\boldsymbol{\omega}}_{\mathcal{B}/\mathcal{N}} = \boldsymbol{L}_B - m_{\text{P}}[\tilde{\boldsymbol{r}}_{F_c/B}]\boldsymbol{r}^{''}_{F_c/B} - \Big([I^{'}_{\text{sc},B}] + [\tilde{\boldsymbol{\omega}}_{\mathcal{B}/\mathcal{N}}][I_{\text{sc},B}]\Big)\boldsymbol{\omega}_{\mathcal{B}/\mathcal{N}} \\ - \Big([I^{'}_{\text{P},F_c}] + [\tilde{\boldsymbol{\omega}}_{\mathcal{B}/\mathcal{N}}][I_{\text{P},F_c}]\Big)\boldsymbol{\omega}_{\mathcal{F}/\mathcal{B}} - [I_{\text{P},F_c}]\boldsymbol{\omega}^{'}_{\mathcal{F}/\mathcal{B}} - m_{\text{P}}[\tilde{\boldsymbol{\omega}}_{\mathcal{B}/\mathcal{N}}][\tilde{\boldsymbol{r}}_{F_c/B}]\boldsymbol{r}^{'}_{F_c/B} \end{aligned} \tag{28}$$

Equation (27) is the translational equation of motion for the spacecraft hub point B with respect to the inertial frame. This vector equation is frame-independent and general so that it can represent a wide range of spacecraft configurations chosen for software implementation. Equation (28) is the rotational equation of motion for the spacecraft system. Note that although the prescribed gimbal states are not directly present in Eq. (27) or (28), they are incorporated into several of the existing variables.[12]

NUMERICAL SIMULATION

The validity of the formulation developed in this work is demonstrated through a numerical simulation scenario. Fortunately, there are a wide variety of prescribed motion actuator scenarios that can be considered for the simulation. This work can be applied to actuated spacecraft components or even robotic components independent from the space domain. Robotic manipulator arms, actuated motion platforms, servo-ed sensors or cameras, gimbal thrusters, and articulated solar arrays are just a few examples of objects whose motion can be purely prescribed using the formulation developed in this work.

The application of interest chosen to simulate in this work is a spacecraft gimbal thruster, where the body-frame relative thrust direction is commanded. Gimbal actuators often have a limited range of pointing motion; where both the gimbal tip and tilt angles are given upper and lower bounds. In this simulation, the gimbal pointing range is chosen to be $-25^{\circ} \leq \psi \leq 25^{\circ}$ and $-30^{\circ} \leq \phi \leq 30^{\circ}$.

Table 4. Simulation setup parameters.

Parameter	Value	Unit
Δt	1	sec
$\Delta\theta$	0.5	deg
$\delta\theta$	2.0	deg
α_{max}	2.0	deg/s^2
n_{s_1}	256	steps
n_{s_2}	256	steps
θ_{0_1}	0.0	deg
θ_{0_2}	0.0	deg
θ_{f_1}	128.0	deg
θ_{f_2}	128.0	deg
ψ_0	25.0	deg
ϕ_0	0.0	deg
ψ_f	-25.0	deg
ϕ_f	0.0	deg

The simulation sets up a gimbal thruster platform that is initially operating at one extreme of its pointing range ($\psi_0 = 25.0^\circ, \phi_0 = 0.0^\circ$). The corresponding motor angles are zero for this initial gimbal attitude. The chosen gimbal reference attitude is at the opposite end of the gimbal's operating range, where both stepper motors must rotate by 128 degrees to achieve the desired attitude. Motor 1 is commanded to move first, followed by motor 2. The simulation setup parameters are shown in Fig. (4).

Note that 512 motor steps are required for the gimbal to complete the desired attitude motion. For such an extensive simulation, it is very difficult to view the stepper motor angle rate and acceleration profiles. For this reason, Fig. (6) presents a simplified scenario where each motor completes only ten steps. As is expected, the motors' angle, angle rate, and acceleration profiles are indicative of the bang-bang acceleration profile described in this work. The simulation results for the desired attitude pointing scenario are presented in Figs. (7-10) below. Figure (7) depicts the sequential stepper motor motion across the entire simulation period. Motor 2 is seen to remain at rest while motor 1 completes the required motion, and vice versa. Fig. (8) presents the time history of the thruster's prescribed states. To improve the visualization of the gimbal motion, Fig. (9) presents both a two-dimensional and three-dimensional view of the gimbal thruster pointing direction. The red diamond shape seen in Figure (9(a)) represents a typical boundary that delineates the gimbal's allowable pointing range from areas the gimbal cannot actuate to. Figure (10) illustrates the gimbal thruster's initial and final orientations relative to the spacecraft hub.

CONCLUSION

This paper introduces a method of formulating the full rotational kinematic motion of a two-axis gimbal that is actuated sequentially using two stepper motors. Given a series of successive motor step count commands, the presented method analytically determines the motor angles and rates as-

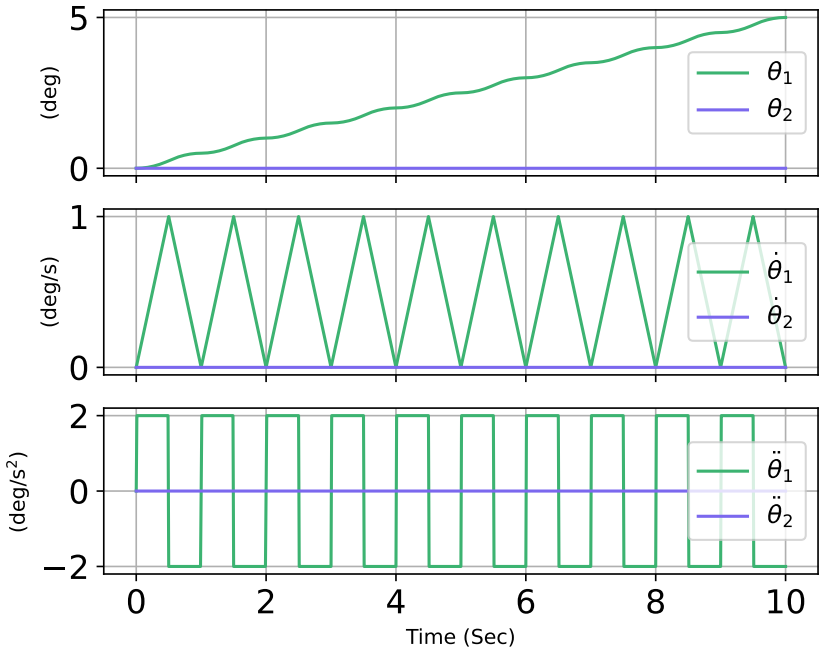

Figure 6. Preliminary stepper motor example scenario.

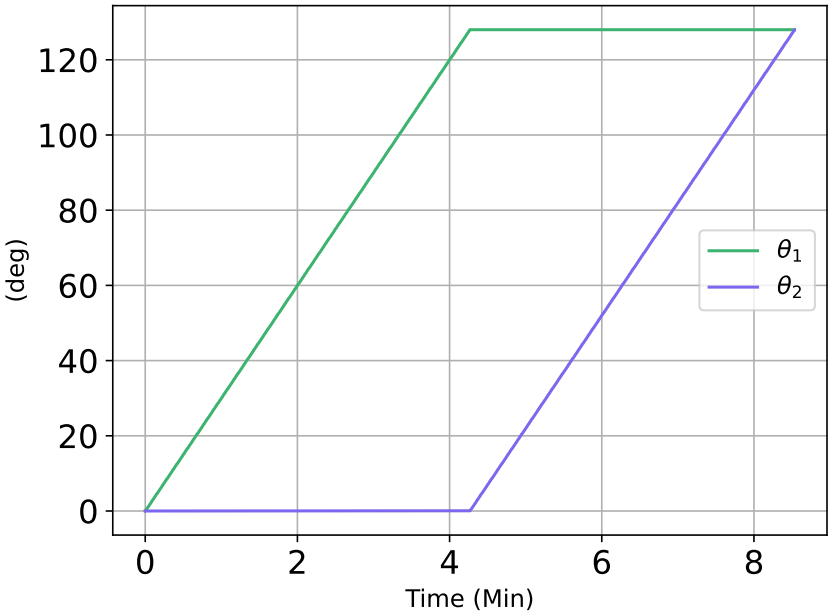

Figure 7. Stepper motor angles.

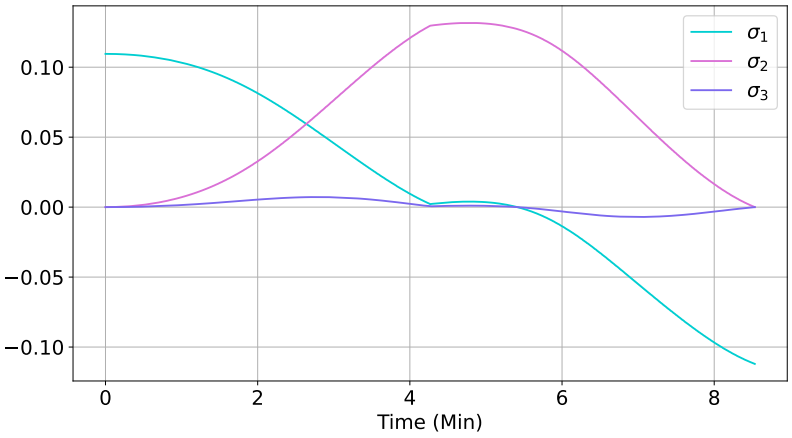

(a) MRP attitude $\boldsymbol{\sigma}_{\mathcal{F}/\mathcal{M}}$.

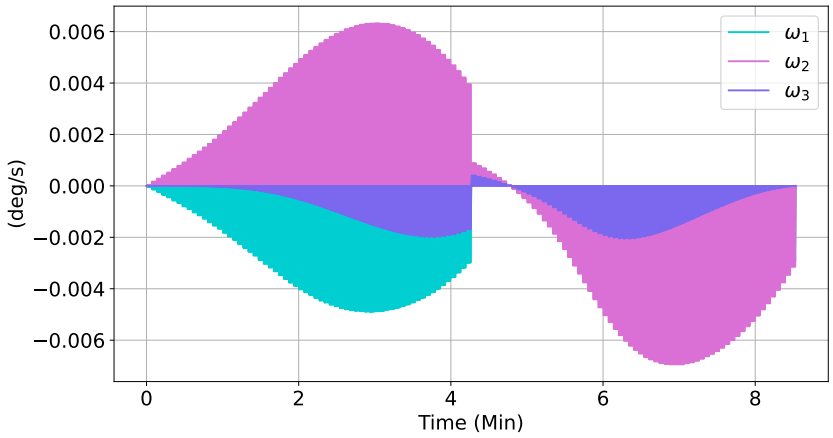

(b) Angular velocity ${}^{\mathcal{F}}\boldsymbol{\omega}_{\mathcal{F}/\mathcal{M}}$.

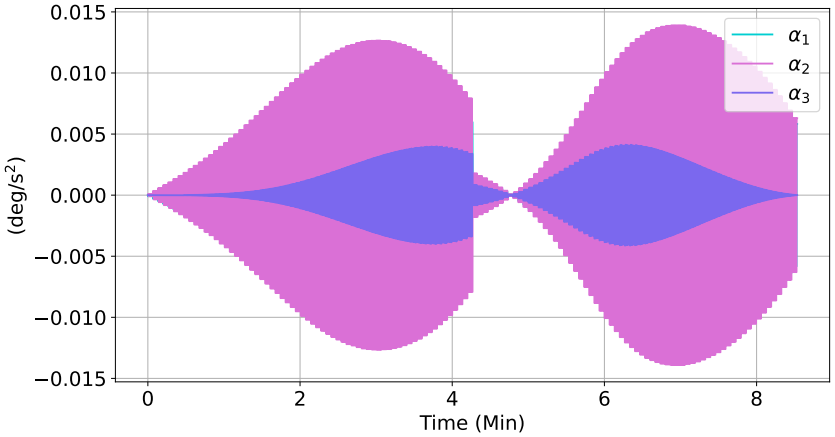

(c) Angular acceleration ${}^{\mathcal{F}}\boldsymbol{\omega}'_{\mathcal{F}/\mathcal{M}}$.

Figure 8. Gimbal prescribed states.

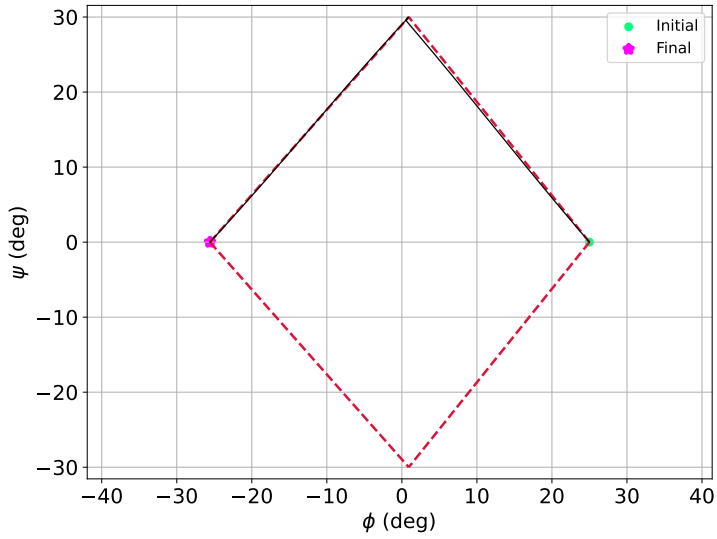

(a) 2D pointing trajectory.

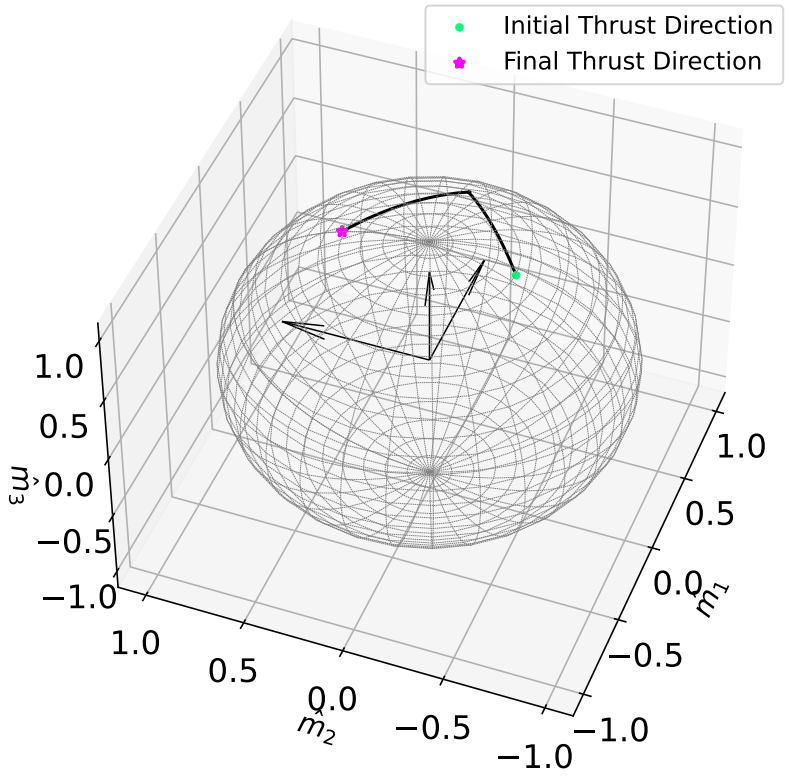

(b) Thrust direction.

Figure 9. Gimbal pointing trajectory.

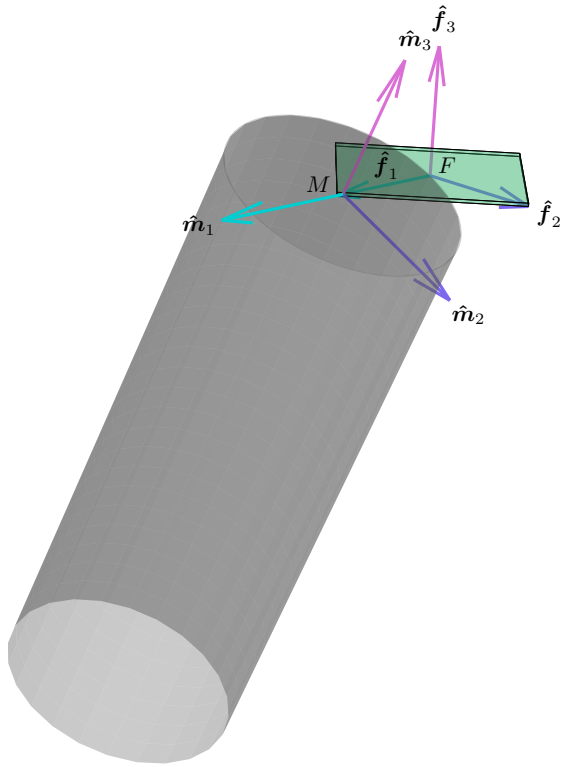

(a) Initial

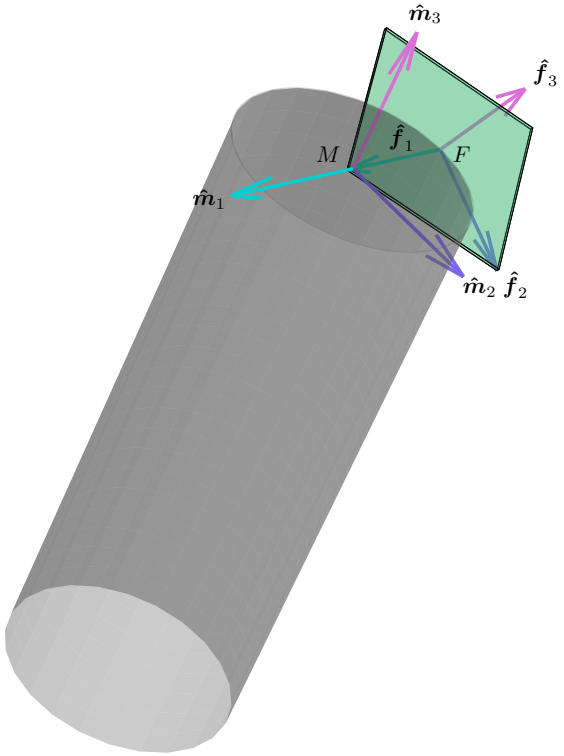

(b) Final

Figure 10. Initial and final gimbal orientations.

suming a bang-bang acceleration profile for each step. The corresponding gimbal tip and tilt angles, PRP attitude trajectory, principal angle rates, and accelerations are determined using a provided gimbal manufacturer lookup table and linear interpolation as needed. The method of determining the gimbal's prescribed kinematic rotational states is presented. Accordingly, the prescribed gimbal state trajectory can be readily implemented into a spacecraft dynamics simulation to conduct any desired system dynamics analysis. Future work will investigate simultaneous motor actuation and expand the analysis to incorporate the stepper motors' effect on the gimbal's translational motion. Future work will also include creation of a gimbal actuator module in Basilisk to interface with the existing prescribed motion dynamics module in order to simulate a full spacecraft dynamics scenario.

REFERENCES

[1] C. Allard, H. Schaub, and S. Piggott, "General Hinged Rigid-Body Dynamics Approximating First-Order Spacecraft Solar Panel Flexing," *Journal of Spacecraft and Rockets*, Vol. 55, No. 5, 2018, pp. 1290–1298.

[2] D. Y. Oh, S. Collins, T. Drain, W. Hart, T. Imken, K. Larson, D. Marsh, D. Muthulingam, J. S. Snyder, D. Trofimov, *et al.*, "Development of the Psyche mission for NASA's Discovery Program," 2019.

[3] A. Jain and G. Rodriguez, "Recursive Dynamics Algorithm for Multibody Systems with Prescribed Motion," *Journal of Guidance, Control, and Dynamics*, Vol. 16, No. 5, 1993, pp. 830–837.

[4] R. McGregor and L. Oshinowo, "Flight 6A: Deployment and Checkout of the Space Station Remote Manipulator System (SSRMS)," 6th International Symposium on Artificial Intelligence and Robotics and Automation in Space: i-SAIRAS 2001, Canadian Space Agency, St-Hubert, Quebec, Canada, June 18-22, 2001.

[5] R. Kristiansen and D. Hagen, "Modelling of actuator dynamics for spacecraft attitude control," *Journal of Guidance, Control, and Dynamics*, Vol. 32, No. 3, 2009, pp. 1022–1025.

[6] R. W. Aldhaheri and H. K. Khalil, "Effect of unmodeled actuator dynamics on output feedback stabilization of nonlinear systems," *Automatica*, Vol. 32, No. 9, 1996, pp. 1323–1327, https://doi.org/10.1016/0005-1098(96)00077-5.

[7] M. S. Mahmoud and H. K. Khalil, "Robustness of high-gain observer-based nonlinear controllers to unmodeled actuators and sensors," *Automatica*, Vol. 38, No. 2, 2002, pp. 361–369, https://doi.org/10.1016/S0005-1098(01)00253-9.

[8] H. K. Khalil, "A note on the robustness of high-gain-observer-based controllers to unmodeled actuator and sensor dynamics," *Automatica*, Vol. 41, No. 10, 2005, pp. 1821–1824, https://doi.org/10.1016/j.automatica.2005.04.008.

[9] J. Denavit and R. S. Hartenberg, "Kinematic modeling for robot calibration," *Trans ASME J Appl Mech 22*, 1995, pp. 215–221.

[10] E. G. Rafael Arnay, Javier Hernández-Aceituno and L. Acosta, "Teaching kinematics with interactive schematics and 3D models," *Computer Applications in Engineering Education*, Vol. 25, No. 3, 2017, pp. 420–429.

[11] R. W. Longman, R. E. Lindbergt, and M. F. Zedd, "Satellite-mounted robot manipulators—New kinematics and reaction moment compensation," *The International Journal of Robotics Research*, Vol. 6, No. 3, 1987, pp. 87–103.

[12] L. Kiner, J. V. Carneiro, C. Allard, and H. Schaub, "Spacecraft Simulation Software Implementation of General Prescribed Motion Dynamics of Two Connected Rigid Bodies," AAS Rocky Mountain GN&C Conference, Breckenridge, CO, Feb. 2–8, 2023.

[13] G. Bascom, L. Kiner, and H. Schaub, "Spacecraft Dynamics Analysis Using Stochastic Point-Mass Model of Human Motion," AAS/AIAA Space Flight Mechanics Meeting, Austin, TX, Jan. 15–19, 2023.

[14] H. Schaub and J. L. Junkins, *Analytical Mechanics of Space Systems*. Reston, Virginia: American Institute of Aeronautics and Astronautics, Inc., 4 ed., 2018.